Modification of the secondary-electron spin polarization in Co/Cu(110) films via gaseous adsorbates

Robert M. Reeve,* Shin-Liang Chin, Adrian Ionescu, and Crispin H. W. Barnes
Cavendish Laboratory, University of Cambridge, JJ Thomson Avenue, Cambridge CB3 0HE, United Kingdom
(Received 12 September 2011; published 28 November 2011)

The effect of O and N adsorbates on the magnetic properties of ultrathin Co/Cu(110) films was investigated *in situ* by measuring the spin polarization of secondary electrons emitted from the surface using Mott polarimetry. The data have been fitted to a function to take into account the exponential attenuation of the signal through the layers above, yielding a room temperature paramagnetic-ferromagnetic transition thickness of $d_c = 3.5 \pm 1.0$ monolayers (ML). This evolution was compared to the equivalent evolution for cobalt films grown on O- and N-saturated surfaces. In the case of nitrogen, the onset of ferromagnetism occurs at a thickness of 4.9 ± 0.5 ML and the saturation polarization is reduced to 65% of the value for the bare cobalt film, implying a dramatic quenching of the magnetic moment in the uppermost layer of the films. For films grown on the oxygen surface, a change in growth mode from three-dimensional to layer-by-layer growth dominates the behavior and this leads to a decrease in d_c to 2.3 ± 0.3 ML and a 38% increase in the saturation polarization value.

DOI: 10.1103/PhysRevB.84.184431 PACS number(s): 75.70.Rf, 68.43.−h, 75.50.Cc, 75.70.Ak

I. INTRODUCTION

The study of gases adsorbed to transition metal surfaces has received considerable attention from both an experimental and theoretical standpoint due to the ability to modify a system's surface properties (morphology,[1,2] electronic structure,[3] stress,[4] optical properties,[5,6] *etc*) by the addition of small quantities of different atomic and molecular species at the film interface. An understanding of these interactions is also vital for industrially relevant catalytic processes, a case in point being CO and H_2 on Co/Fe surfaces in Fischer-Tropsch synthesis.[7–9]

More recently, experimental studies have begun to investigate the effects of gaseous adsorbates on magnetic systems with a view to manipulating the magnetic properties down to the atomic scale through the tailoring of the surface. Gaseous adsorbates have been demonstrated to change the coercivity of films[10,11] and are not only able to affect the magnitude of the magnetization in such systems[12–14] but also its direction.[15–19] A striking example of this is the 90° in-plane spin-reorientation transition (SRT) in Co/Cu(110) films, caused by a fraction of a monolayer of CO and no other known gas.[20] It has also recently been demonstrated that the Kondo effect can be modified in the vicinity of a single molecule of cobalt phthalocyanine by controlling the chemical environment of the Co ion.[21]

The theoretical modeling of such systems presents a greater challenge than for nonmagnetic systems, however, researchers have started to predict the electronic hybridization of these adsorbates with the surface atoms that lead to changes in the magnetic moment[3,22–26] and magnetic anisotropy energy[18] at a first-principles level using approaches such as density functional theory (DFT). It has recently been predicted, for example, that in monotonic Fe wires that grow on Ir(100) surfaces, the exchange interaction between the Fe atoms can be switched from antiferromagnetic to ferromagnetic by changing the H coverage.[27] For the above work, an isolated wire was modeled as a simplification to the experimentally realized Fe-Ir-Fe sandwich structures. This highlights a quite general problem, namely, that it is often difficult to directly compare the results of experiment and theory and in many cases comparative experimental data to test theoretical predictions of these changes in magnetic properties are completely lacking.

We have previously studied the effect of oxygen and nitrogen adsorbed to thin magnetic films of Co/Cu(001) using Mott polarimetry, which naturally lends itself to such adsorbate studies due to the extreme surface sensitivity of secondary electron emission.[12] Co/Cu films have received a lot of attention in the past due to their potential in GMR-type superlattice structures,[28] making them an excellent choice for a comparative study, with Co/Cu(001) being an archetypal system due to the almost perfect layer-by-layer growth mode.[29] The polarimeter measures the secondary electron spin-polarization (SESP), which we have shown can be readily related to the spin splitting of the band structure and provides excellent agreement with the predictions of first-principles DFT calculations,[13] providing a link between the microscopic theory and the macroscopically observed SESP. The effects are found to be chemically selective for this system, with oxygen hardly modifying the saturation polarization, yet nitrogen reducing this quantity to 80% of the value for uncovered films.

In the present study, we extend the work to the less studied Co/Cu(110) system to investigate the impact of morphology on the SESP. While Co on Cu(001) grows in an almost perfect layer-by-layer fashion, the inherently corrugated Cu(110) surface leads to a 3D growth mode with islands forming that are preferentially elongated along the $[1\bar{1}0]$ direction.[30] In thin films, below about 15 monolayers (ML), the magnetocrystalline contribution to the anisotropy is found to be negligible[31] with the films displaying a primarily uniaxial anisotropy rendering the magnetic easy axis along the [001] direction. The system evolves in time due to the adsorption of residual CO on the surface, modifying the net anisotropy and resulting in a 90° in-plane SRT. This transition can also be observed in the SESP signal,[32] however, extended exposure of the films to an electron beam can locally reverse the switch by dissociating the CO.[32,33] This effect has recently been quantitatively modeled to extract the electronic cross section for the process and shows that only 0.065 ML of CO are responsible for the switch.[33] Overlayers such as Cu from deposition and annealing[34] or adsorbates such as oxygen on the surface[30] can also prevent the SRT from occurring,

by sitting in the preferential adsorption sites for the carbon monoxide. Furthermore, for cobalt grown on the oxygen reconstructed surface, the growth mode can also be modified, changing the balance of anisotropy contributions responsible for the effect.[30,35,36] The effect of these morphology changes on the SESP is investigated here, with the results compared to Co/Cu(001) films.

II. EXPERIMENTAL

All experiments were performed *in situ* in an ultrahigh vacuum (UHV) chamber with a base pressure of 4×10^{-10} mbar. The substrate is a single copper (110) crystal mounted on a custom-built sample manipulator that includes sample heating and biasing facilities. The crystal was prepared via 1.5 kV Argon ion sputtering and 770 K annealing cycles until it was suitably contaminant free and well ordered, as indicated using low energy electron diffraction (LEED) and Auger electron spectroscopy (AES). The LEED and AES measurements were performed using a combined *SPECS* ErLEED 150 instrument. The Auger scans were also used to measure the film thicknesses by comparing the peak heights from the substrate and overlayer, a technique that carries an error of around 15%. For gas dosing, the research grade gases were admitted to the chamber via a leak valve to a pressure a few orders of magnitude above the base pressure, for an appropriate time to provide the desired exposure. For the growth of bare cobalt films, residual oxygen was removed from the surface prior to deposition by exposing the surface to 1000 L ($1\ \mathrm{L} = 10^{-6}$ Torr s) hydrogen at an elevated temperature of 380 K. In the case of the oxygen- and nitrogen-covered films, the substrate was exposed to the respective gases prior to deposition to form specific surface reconstructions. For oxygen, the copper crystal was exposed to 99.9995% purity gas at a pressure of 5×10^{-7} mbar for a period of 30 mins, with the substrate held at 550 K, corresponding to an excess of gas to ensure a saturated surface.[37] With nitrogen, the molecular gas is found not to stick to the surface, therefore the gas was ionized through the sputter gun at a low acceleration voltage of around 400 V. In this case, the gas was admitted to the chamber to a pressure of 4×10^{-6} mbar, with the voltage fine tuned to provide a sample current of 1 μA.[38] The surface was exposed for 30 mins with the temperature held at 620 K to achieve saturation exposure. Cobalt films were deposited at ambient conditions below 300 K, from an *Omicron* EFM3 evaporator using a 99.999% pure rod at a growth rate around 0.5 ML per minute. The Auger peak heights were monitored between growth stages. Magnetic characterization was performed using our 20–25 kV retarding potential Mott polarimeter as described in Ref. 39. A magnetic field was applied across the sample along the [001] axis to provide saturation, which was checked by monitoring *M-H* hysteresis loops of the samples using the magneto-optic Kerr effect (MOKE). For the SESP measurements, data were recorded at remanence.

III. STRUCTURAL CHARACTERIZATION

The LEED images for the copper substrate and cobalt films can be seen at the left side of Fig. 1. The substrate shows clear diffraction spots, indicative of a well ordered crystallographic

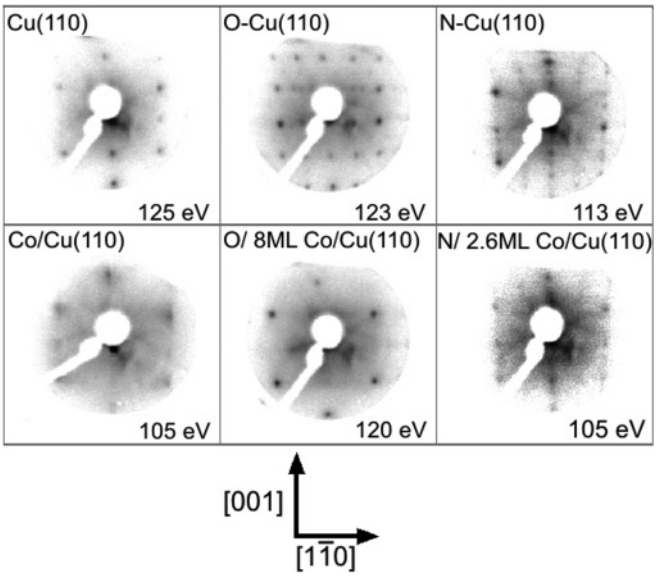

FIG. 1. LEED images of the copper substrate and cobalt films for the different surfaces. The beam energy is shown in the bottom corner of each image. The crystallographic axes are presented in the legend below.

surface. The LEED image for the cobalt film is less distinct due to the 3D growth mode, but still shows clearly discernible spots indicating the films are epitaxial in nature. The LEED spots can be seen to be elongated along the [001] direction, which is consistent with the expected island elongation along the orthogonal axis.[40] The right of the figure presents LEED images showing the various surface reconstructions for the different systems. Exposure of the bare Cu(110) surface to oxygen leads to an ordered (2×1) reconstruction corresponding to 0.5 ML O coverage.[37,41] For Co growth on the oxygen saturated surface, it has been explained that the adsorbate can act as a surfactant, changing the growth mode of the system to a more layer-by-layer 2D fashion.[35,36] The surface of the oxygen-saturated Co film is known to form a (3×1) reconstruction.[30,36] Since this corresponds to a greater surface coverage of oxygen than for the Cu surface, formation of this structure is facilitated if oxygen is admitted to the chamber during Co deposition.[37,42,43] Comparing the clean Cu(110) surface to the oxygen-exposed substrate it can clearly be seen that the periodicity of spots along the [1$\bar{1}$0] direction has doubled, indicative of the formation of a Cu(110) (2×1)-O surface reconstruction as expected. The LEED patterns following the subsequent deposition of 8 ML of Co are shown in the next row. Were the cobalt surface saturated, the (3×1) reconstruction would be expected, however, the amount of oxygen on the surface is not sufficient to allow this to form in the work here. Instead, a diffuse pattern is seen where only the primary spots are visible, in qualitative agreement with the study of Ling *et al.* In the case of nitrogen, the bare copper surface can be seen to undergo a (2×3) reconstruction, in agreement with reports in the literature for such a surface.[38,44] This structure could correspond to just 1/6 ML surface N.[45] The pattern for the 2.6 ML Co film is less distinct, but retains streaked features along the [001] axis, similar to the results of Ma *et al.* for low Co coverage.[38] In

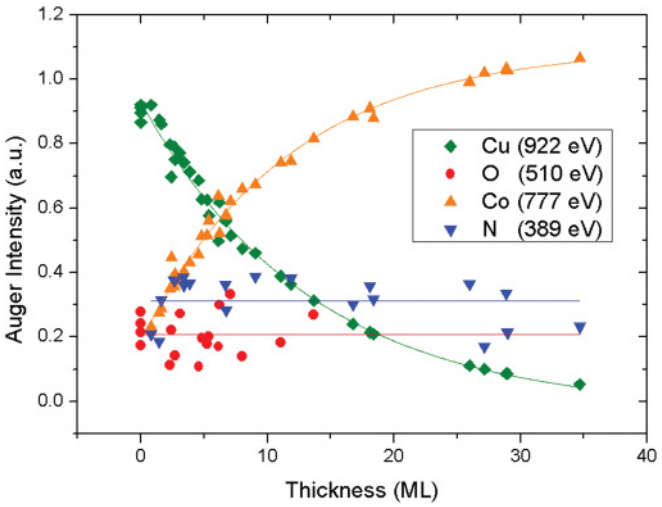

FIG. 2. (Color online) The evolution of Auger peak heights with cobalt thickness for cobalt grown on oxygen and nitrogen reconstructed copper surfaces, compiled over several growth runs. The AES signal is plotted relative to the bare copper peak height in each case. The gas peak remains roughly constant as the cobalt increases and copper decreases. The lines are guides for the eye.

order to monitor the chemical evolution of the films during deposition, AES peak heights were recorded for the species of interest as shown in Fig. 2. With thickness, the cobalt peak height can be seen to grow at the expense of the peak from the copper substrate. Meanwhile, the gas peaks remained roughly constant displaying no particular trend or systematic decrease, supporting the assertion that the quantity of each gas remains constant, as has been seen in previous studies.[12]

IV. MAGNETIC CHARACTERIZATION

The change in *M-H* loop coercivity, measured using MOKE, is presented in Fig. 3. The bare Co/Cu(110) system is known to evolve in time due to the adsorption of residual CO gas onto the surface,[20,32,46] with the coercivity gradually reducing to zero over a few hours (depending on the exact partial pressure of CO gas in the chamber) as a 90° in-plane SRT occurs. Since the MOKE measurements take several minutes to perform, the data points for these bare cobalt films all correspond to different samples to reduce the potential for systematic error due to the residual gas. For the gas-covered surfaces no such SRT is found to occur[47] and therefore the data correspond to incremental growth steps for the same sample. In each case, the films do not display any coercivity at low thickness. In the bulk, cobalt has a Curie temperature high above room temperature (RT), however, the case is different in thin films. For the Co/Cu(001) system, for example, Miguel *et al.* report a linear increase in Curie temperature from 150 K in 1.5 ML films toward 1388 K in samples over 5 ML in thickness.[48] As such, for a particular growth temperature, you can expect a film to undergo a paramagnetic-to-ferromagnetic percolation phase transition at a characteristic layer thickness. For the oxygen-covered films, the coercivity is seen to rise at a very fast rate as a function of thickness, exceeding the value that can be applied by the Helmholtz coil during MOKE measurements by a thickness of about 5 ML. For the other two cases, the same general trend can be seen with the coercivity initially increasing as a function of thickness and then reducing somewhat for the thickest films, although the maximum coercivity is larger for the bare cobalt films than for the nitrogen surface. The thickness evolution in SESP for the bare cobalt film has been plotted in the center of Fig. 4. The normalized polarization is observed to asymptotically approach a saturation value as an ever greater thickness of film is being probed, until the point that only the top of the films is contributing to the signal. There is an initial delay in the onset of ferromagnetism at low thicknesses where the

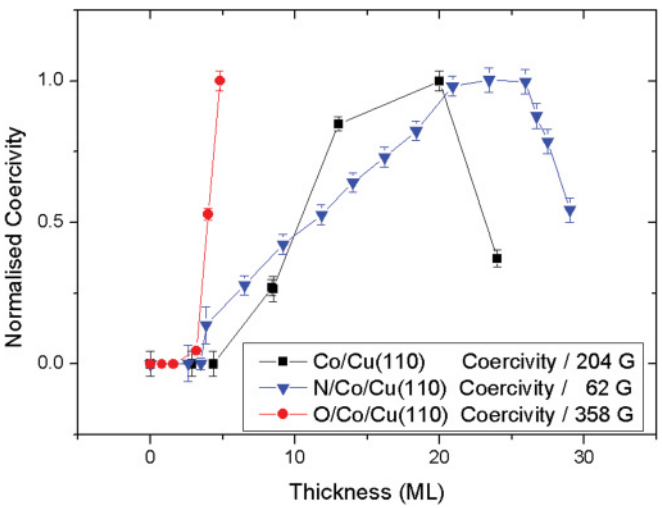

FIG. 3. (Color online) A graph showing the thickness evolution of the *M-H* loop coercivity, measured using MOKE, for the bare cobalt and gas-covered films. The coercivity has been normalized with respect to the maximum value for each type of sample, as indicated in the legend. The lines are guides for the eye.

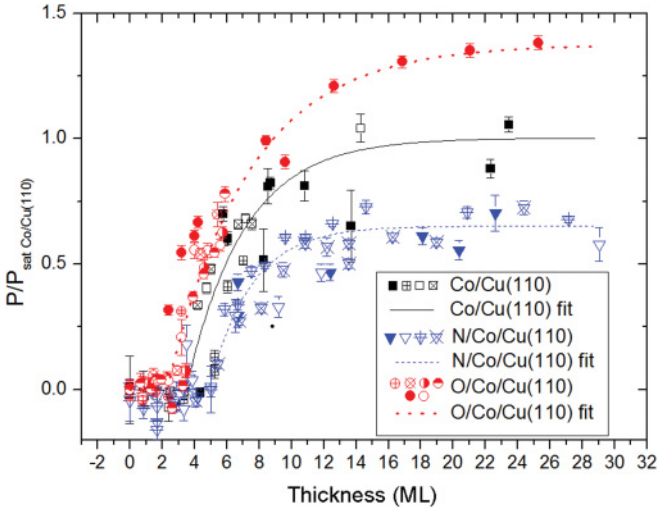

FIG. 4. (Color online) A graph showing the thickness evolution of the SESP for the different surfaces. The polarization has been normalized with respect to the saturation polarization for the uncovered surface, $P_{s,\mathrm{Co}}$, in each case. The lines represent fits to the data as described in the text. Different style data points correspond to different experimental runs. In the case of Co, the solid square data set is compiled from separate time evolution experiments.

TABLE I. A table presenting the best fit parameters for the thickness evolution of SESP for the bare cobalt and adsorbate-covered films. Here, d_c is the critical thickness for the onset of ferromagnetism, P_s is the saturation polarization, and λ is the information depth.

Surface	d_c/ML	$P_s(\%)$	$P_s/P_{s,\mathrm{Co}}$	λ/ML
Co	3.5 ± 1.0	10.9 ± 1.8	1.00	3.6 ± 1.5
N	4.9 ± 0.5	7.1 ± 0.5	0.65	2.6 ± 0.4
O	2.3 ± 0.3	15.0 ± 1.1	1.38	5.1 ± 0.5

Curie temperature of the films is expected to be below room temperature. The above features can be incorporated into the following function, which has been used to fit the polarization, P, as a function of film thickness, d, as we have shown previously for the Co/Cu(001) system:[12]

$$P(d) = P_s\left[1 - \exp\left(-\frac{d - d_c}{\lambda}\right)\right]. \quad (1)$$

Here, d_c is the critical thickness for the paramagnetic-to-ferromagnetic percolation phase transition, λ is the information depth and P_s is the saturation polarization. The parameters for the fit can be found in the first row of Table I. The onset of ferromagnetism is found to occur at a critical thickness of 3.5 ± 1.0 ML, larger than the value of 1.6 ± 0.1 ML found for the Co/Cu(001) system, which is to be expected, since the 3D growth mode in the present system will delay the percolation of the film. In the literature there is a wide range of values for this parameter, from 2.3 to 11 ML, with the present value in the middle of the range.[38,43,46,49] The value of P_s is found to be $10.9 \pm 1.8\%$, which is larger than the value of $7.9 \pm 0.1\%$ found for the Co/Cu(001) system. This is because in that work the polarization was measured along the hard magnetic axis, whereas here the polarization is measured along the easy axis, with the films measured at remanence in each case. The information depth is found to be 3.6 ± 1.5 ML, in excellent agreement with the previous study. The comparison of the thickness evolution in SESP for the films grown on the reconstructed surfaces, as compared to the bare cobalt film, is also presented in Fig. 4 with the polarization normalized with respect to the saturation polarization for the uncovered surface, $P_{s,\mathrm{Co}}$, in each case. In the case of oxygen, for films thicker than about 5 ML, the coercivity was larger than 450 G, the largest value that the Helmholtz coil can generate with a continuous current. As such, for these data points, MOKE was not carried out and the maximum pulsed field of 700 G was applied across the samples for SESP measurements. The data in each case have been fitted to Eq. (1), which can be seen to fit the data well and the parameters for the fits can also be found in Table I. For the nitrogen films, d_c is delayed with respect to the uncovered surface to 4.9 ± 0.5 ML and P_s is reduced to $7.1 \pm 0.5\%$, which is a 35% reduction over the value for Co/Cu(110) surfaces. Conversely, in the case of oxygen, d_c occurs at a lower thickness of 2.3 ± 0.3 ML and P_s is enhanced by 38% to $15.0 \pm 1.1\%$. The values of λ are found to be 5.1 ± 0.5 ML for oxygen and 2.6 ± 0.4 ML for nitrogen.

V. DISCUSSION

In each experimental run, no MOKE signal was detected when the SESP signal was also zero, thereby providing an independent measurement of the onset of ferromagnetism. The observed delay in ferromagnetic onset for the nitrogen system is in contrast to the predictions of York and Leibsle[44] and the work of Ma *et al.*,[38] who observe it to occur at a lower thickness as compared to bare surfaces, however, there is considerable uncertainty as to the actual value of d_c for the bare system, which could well arise due to the intense sensitivity of the system to CO. The delay observed here is in line with that previously observed for the Co/Cu(001) system.[12] Conversely, in the case of the oxygen-covered films, a flattening of the surface may be expected, which explains why we have a lower value of d_c in this case as 2D behavior is more closely followed. The most noticeable difference between the films is the different values of the saturation polarization. To assess how a measured polarization signal may be affected by changes in surface magnetic moment, a simple model is adopted based on that employed by Pick and Dreyssé[50] and previously employed for Co/Cu(001) films.[12] Whilst the approximation of a flat surface is clearly a vast simplification, the comparison of the predictions here to those of the previous system and to the existing DFT calculations for the ideal surface arrangement can provide insight into the impact of the morphology. The system is modeled as a 7 ML crystal with the effect of the adsorbate assumed to be restricted to changing the magnitude of the magnetic moment of the surface layer, since it is known that such changes in magnetic moment are a direct result of the covalent bond between the species.[22] All other moments are taken as the bulk value at RT, $1.73\,\mu_B$/atom. The polarization signal from each layer, i, is assumed to be proportional to the magnetic moment of cobalt atoms in that layer (p_i) and since we are measuring a change in polarization with respect to the unadsorbate-covered surface, the result is independent of the constant of proportionality. The contribution from each layer is weighted to account for its depth according to the following equation in order to yield the total polarization P from the seven-layer slab:

$$P(7) = \sum_{i=0}^{6}\left[p_i \exp\left(-\frac{i}{\lambda}\right)\right]. \quad (2)$$

The moment of the uppermost layer for the adsorbate system is varied until the ratio of the polarization from adsorbate-covered system to the bare cobalt film, $P_{S\mathrm{ads}}/P_{S_0}$, matches the experiment. A representative value of the information depth, λ, equivalent to 3 ML has been used in the calculations, as before.[13] In order to reproduce the experimental results for N, a complete quenching of the magnetic moment in the uppermost layer is required, a much greater effect than for the Co/Cu(001) system, which could be due to an increased coordination of the N atoms to the cobalt surface. The effect of various p-block adsorbates on the magnetic properties of ferromagnetic surfaces has recently been studied at an *ab initio* level by Gunn and Jenkins using DFT.[3] For 0.5 ML N coverage, they find that the surface magnetic moment is suppressed to $1.41\,\mu_B$/atom due to a reduction in majority and increase in minority occupation in the surface-layer d

band. Again, such a decrease in moment is qualitatively in agreement with our observations. The greater extent of the suppression observed in the experiments is likely to arise due to the simplified assumptions used in both the above model and the DFT calculations, which do not attempt to take into account the film morphology realized in practice. In order to further assess this impact of morphology, we can extend the calculation above to also include an adsorbate-induced reduction of the magnetic moment in the second layer due to directly-bonded nitrogen at step edges. If we assume that the reduction in this second layer is a third of that at the surface,[51] then the calculated surface magnetic moment decrease is less, as expected, but these moments are still dramatically reduced to $0.2 \pm 0.5\,\mu_B$. The magnetic moment per atom in the second layer is correspondingly $1.2 \pm 0.2\,\mu_B$. While the reduction of the uppermost magnetic moments may be further subdued if the exact surface morphology was simulated and the effect of adsorbate-induced demagnetization was included in all layers, the magnitude of the reduction implies that the nitrogen-induced magnetic moment suppression is inherently greater in this system than for Co/Cu(001), even taking into account morphology differences.

In the case of the oxygen surface, if the increase of the saturation polarization were due to solely the hybridization of the Co atoms and the O adatoms, the model of Eq. (2) predicts a marked increase in the surface magnetic moment to $3.8 \pm 0.8\,\mu_B$/atom. However, there is also a significantly different growth mode between the bare and oxygen-covered films, which is expected to be the primary cause of the increased SESP, since for the (001) surface, oxygen was found to have little impact on the polarization. In the Co/Cu(110) systems with a 3D growth mode, more copper segregation is known to occur and this will increase the number of unpolarized secondary electrons emitted and thereby reduce the measured polarization.[40] The increase in criticial thickness and decrease in saturation polarization for the nitrogen films implies that an equivalent decrease in copper segregation is not occuring in this case. Another potential contribution to the different behavior in the oxygen films is suggested by the DFT work of Gunn and Jenkins, which intriguingly predicts that O adatoms on Co(110) may themselves couple ferromagnetically to the surface, gaining a magnetic moment of $0.26\,\mu_B$ in the case of 0.5 ML coverage, while there is little change to the uppermost cobalt moments.[3] It is therefore possible that this effect may also be partly responsible for the enhanced polarization values observed here.

VI. CONCLUSIONS

In summary, we have studied the effect of O and N on the thickness evolution in Co/Cu(110) films and compared it to that for Co/Cu(001) heterostructures. The Co/Cu(110) system presents a far greater challenge due to the inherent time evolution in properties for the bare system with residual CO adsorption and due to its 3D growth mode. For growth on the nitrogen reconstructed surface, a delay in the onset of ferromagnetism and reduction in surface magnetic moment is observed with respect to the bare film, in line with the previous work. The magnitude of this reduction is seen to be much larger, implying a dramatic quenching of the surface magnetic moments. For growth on the oxygen covered surface, the reverse is seen, with the onset of ferromagnetism occuring at a lower thickness than for the bare film and with a larger saturation polarization. In this case, the oxygen is known to have a surfactant effect, leading to smoother films with less copper segregation, which explains the observed results. Future work is needed to properly model these systems at a first-principles level. While previous work has used DFT to look into the effect of such adsorbates on the crystallographic Co(110) surfaces, it has been shown here that the nonideal growth modes can have a radical impact on experimentally measured properties.

ACKNOWLEDGMENTS

The authors would like to thank the EPSRC for studentship funding and the Cambridge Philosophical Society for additional financial support.

*robert.reeve@cantab.net

[1] L. Guillemot and K. Bobrov, Phys. Rev. B **83**, 075409 (2011).
[2] X.-Q. Zhang, W. K. Offermans, R. A. van Santen, A. P. J. Jansen, A. Scheibe, U. Lins, and R. Imbihl, Phys. Rev. B **82**, 113401 (2010).
[3] D. S. D. Gunn and S. J. Jenkins, Phys. Rev. B **83**, 115403 (2011).
[4] M. K. Bradley, D. P. Woodruff, and J. Robinson, Phys. Rev. B **84**, 075438 (2011).
[5] A. V. Gavrilenko, C. S. McKinney, and V. I. Gavrilenko, Phys. Rev. B **82**, 155426 (2010).
[6] P. D. Lane, G. E. Isted, and R. J. Cole, Phys. Rev. B **82**, 075416 (2010).
[7] E. Iglesia, Appl. Catal., A **161**, 59 (1997).
[8] J. Cheng, P. Hu, P. Ellis, S. French, G. Kelly, and C. Martin Lok, Top. Catal. **53**, 326 (2010).
[9] X. Gong, R. Raval, and P. Hu, Surf. Sci. **562**, 247 (2004).
[10] D. Küpper, A. Ionescu, S. Easton, H. Kurebayashi, and J. A. C. Bland, J. Appl. Phys. **103**, 07C911 (2008).
[11] J. Bansmann, M. Getzlaff, C. Westphal, and G. Schönhense, J. Magn. Magn. Mater. **117**, 38 (1992).
[12] K. P. Kopper, D. Küpper, R. Reeve, T. Mitrelias, and J. A. C. Bland, J. Appl. Phys. **103**, 07C904 (2008).
[13] K. P. Kopper, D. Küpper, R. Reeve, T. Mitrelias, D. S. D. Gunn, and S. J. Jenkins, Phys. Rev. B **80**, 052406 (2009).
[14] C. Sorg, N. Ponpandian, M. Bernien, K. Baberschken, H. Wende, and R. Q. Wu, Phys. Rev. B **73**, 064409 (2006).
[15] H. Abe, K. Amemiya, D. Matsumura, J. Miyawaki, E. O. Sako, T. Ohtsuki, E. Sakai, and T. Ohta, Phys. Rev. B **77**, 054409 (2008).
[16] D. Matsumura, T. Yokoyama, K. Amemiya, S. Kitagawa, and T. Ohta, Phys. Rev. B **66**, 24402 (2002).
[17] W. Weber, C. H. Back, U. Ramsperger, A. Vaterlaus, and R. Allenspach, Phys. Rev. B **52**, R14400 (1995).
[18] S. M. Valvidares, J. Dorantes-Dávila, H. Isern, S. Ferrer, and G. M. Pastor, Phys. Rev. B **81**, 024415 (2010).
[19] T. Nakagawa, H. Watanabe, and T. Yokoyama, Phys. Rev. B **63**, 064409 (2001).

[20]S. Hope, E. Gu, M. Tselepi, M. E. Buckley, and J. A. C. Bland, Phys. Rev. B **57**, 7454 (1998).
[21]A. Zhao, Q. Li, L. Chen, H. Xiang, W. Wang, S. Pan, B. Wang, X. Xiao, J. Yang, J. G. Hou, and Q. Zhu, Science **309**, 1542 (2005).
[22]S. J. Jenkins, Q. Ge, and D. A. King, Phys. Rev. B **64**, 012413 (2001).
[23]P. Błoński, A. Kiejna, and J. Hafner, Surf. Sci. **590**, 88 (2005).
[24]S. Pick, P. Legare, and C. Demangeat, Phys. Rev. B **75**, 195446 (2007).
[25]S. Pick, Surf. Sci. **601**, 5571 (2007).
[26]K. C. Hass, M.-H. Tsai, and R. V. Kasowski, Phys. Rev. B **53**, 44 (1996).
[27]F. R. Vukajlović, Z. S. Popović, A. Baldereschi, and Z. Sljivancanin, Phys. Rev. B **81**, 085425 (2010).
[28]M. J. Hall, B. J. Hickey, M. A. Howson, M. J. Walker, J. Xu, D. Greig, and N. Wiser, Phys. Rev. B **47**, 12785 (1993).
[29]A. K. Schmid and J. Kirschner, Ultramicroscopy **42–44**, 483 (1992).
[30]M. Tselepi, P. J. Bode, Y. B. Xu, G. Wastlbauer, S. Hope, and J. A. C. Bland, J. Appl. Phys. **89**, 6683 (2001).
[31]J. Fassbender, G. Güntherodt, C. Mathieu, B. Hillebrands, R. Jungblut, J. Kohlhepp, M. T. Johnson, D. J. Roberts, and G. A. Gehring, Phys. Rev. B **57**, 5870 (1998).
[32]R. Reeve, S.-L. Chin, K. P. Kopper, A. Ionescu, and C. H. W. Barnes, IEEE Trans. Magn. **47**, 1554 (2011).
[33]R. Reeve, S.-L. Chin, K. P. Kopper, A. Ionescu, and C. H. W. Barnes, Submitted (2011).
[34]S. Hope, E. Gu, B. Choi, and J. A. C. Bland, Phys. Rev. Lett. **80**, 1750 (1998).
[35]C. Tolkes, R. Struck, R. David, P. Zeppenfeld, and G. Comsa, Appl. Phys. Lett. **73**, 1059 (1998).
[36]C. Tölkes, R. Struck, R. David, P. Zeppenfeld, and G. Comsa, Phys. Rev. Lett. **80**, 2877 (1998).
[37]G. Boishin, L. D. Sun, M. Hohage, and P. Zeppenfeld, Surf. Sci. **512**, 185 (2002).
[38]X. D. Ma, T. Nakagawa, Y. Takagi, M. Przybylski, F. M. Leibsle, and T. Yokoyama, Phys. Rev. B **78**, 104420 (2008).
[39]G. C. Burnett, T. J. Monroe, and F. B. Dunning, Rev. Sci. Instrum. **65**, 1893 (1994).
[40]M. T. Kief and W. F. Egelhoff, Phys. Rev. B **47**, 10785 (1993).
[41]L. A. Harris, J. Appl. Phys. **39**, 1419 (1968).
[42]W. L. Ling, O. Takeuchi, D. F. Ogletree, Z. Q. Qiu, and M. Salmeron, Surf. Sci. **450**, 227 (2000).
[43]W. L. Ling, Z. Q. Qiu, O. Takeuchi, D. F. Ogletree, and M. Salmeron, Phys. Rev. B **63**, 024408 (2000).
[44]S. M. York and F. M. Leibsle, Phys. Rev. B **64**, 033411 (2001).
[45]M. Voetz, H. Niehus, J. O'Connor, and G. Comsa, Surf. Sci. **292**, 211 (1993).
[46]S. Hope, Ph.D. thesis, University of Cambridge, 1997.
[47]R. Reeve, Ph.D. thesis, University of Cambridge, 2011.
[48]J. J. DeMiguel, A. Cebollada, J. M. Gallego, S. Ferer, R. Miranda, C. Schneider, P. Bressier, J. Garbe, K. Bethke, and J. Kirschner, Surf. Sci. **211-212**, 732 (1989).
[49]A. Ionescu, Ph.D. thesis, University of Cambridge, 2005.
[50]S. Pick and H. Dreysse, Surf. Sci. **474**, 64 (2001).
[51]From the STM images of the Co/Cu(110) surface of Tselepi *et al.*, it can be very roughly estimated that about a third of adatom sites would be at step edges.[30,52]
[52]M. Tselepi, Ph.D. thesis, University of Cambridge, 2002.